

A HODOSCOPE/SPECTROMETER FOR INTERMEDIATE AND HIGH-ENERGY PHOTONS*

C. A. HEUSCH, R. V. KLINE† and S. J. YELLIN‡

University of California at Santa Cruz, Santa Cruz, California 95064, and California Institute of Technology, Pasadena, California 91109, U.S.A.

Received 16 April 1974

We describe design, construction and testing of, and operational experience with, a detection device for photons of energies from 150 MeV to 1 GeV. The device, which combines Cherenkov radiator and track-chamber elements, attempts to optimize energy resolution and trajectory information for this (difficult)

energy interval. Extension to higher energies is straightforward. Performance characteristics are given from calibration runs and from experience during a major experiment involving heavy backgrounds.

1. Purpose

One of the persisting experimental difficulties in elementary particle physics is the full detection of the kinematical parameters of high-energy photons. While most of the requirements:

- a) high detection efficiency,
- b) precise energy information,
- c) precise trajectory information,
- d) good time resolution,

can be individually met, it is known that simultaneous optimization is very hard. This is true in particular in the energy range between 0.1 and 1 GeV, where opening angles of shower development are non-negligible, photon conversion efficiencies vary widely, and the total number of charged constituents of the electro-

* Work supported in part by the U.S. Atomic Energy Commission under Contract # AT(04-3)-34.
 † Now at Department of Physics, Harvard University, Cambridge, Massachusetts, U.S.A.
 ‡ Now at Department of Physics, University of California, Santa Barbara, Calif., U.S.A.

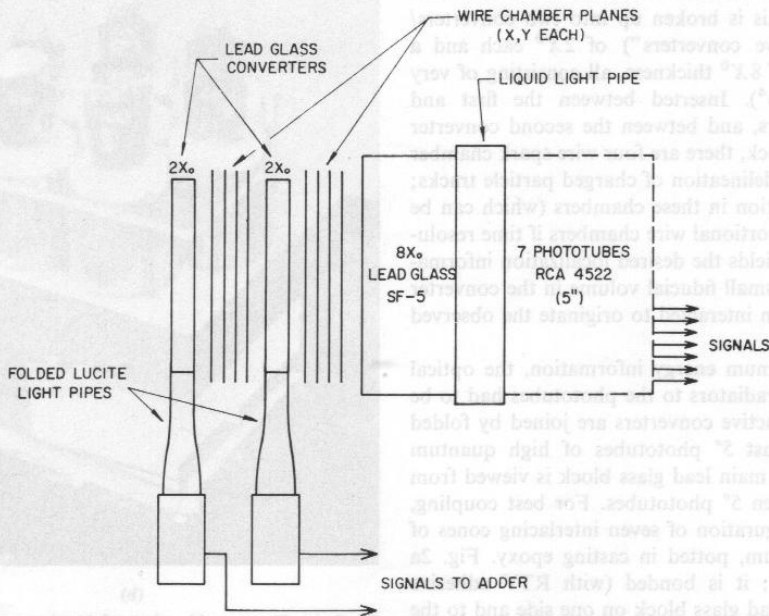


Fig. 1. Schematic sketch of detector. The device can be used with one, two, or more converters/radiators plus subsequent wire (or proportional) chambers.

magnetic cascade is small enough to make statistical fluctuations a major problem.

We report here on construction and use of a detector which tries to maximize the information mentioned under (a)–(d), precisely in this difficult energy range¹). The device was tested and calibrated in a tagged photon beam at the California Institute of Technology 1.5 GeV electron synchrotron. While the energy definition of the parent electron beam was not good enough to check whether the counter was fully optimized, it appears that it comes close.

For use at higher energies, the device can be straightforwardly scaled to contain expected shower energies. Since conversion efficiencies reach a plateau below 1 GeV, there is no further adaptation needed. Rather, the precision in localization and energy measurement increases rapidly²).

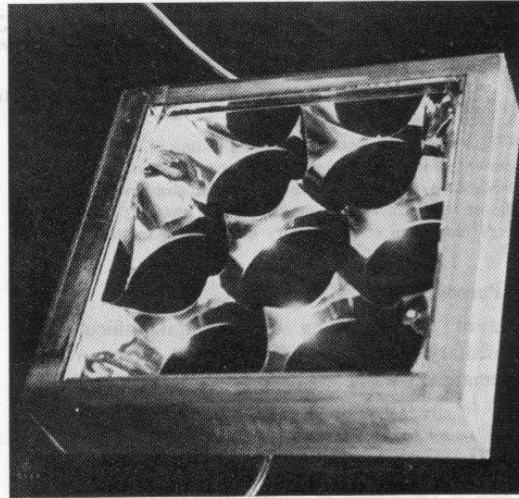
2. Construction of the detector

The detector we built can be varied in many details due to individual experimental requirements without losing its basic features³). We describe here two configurations which we tested in some detail.

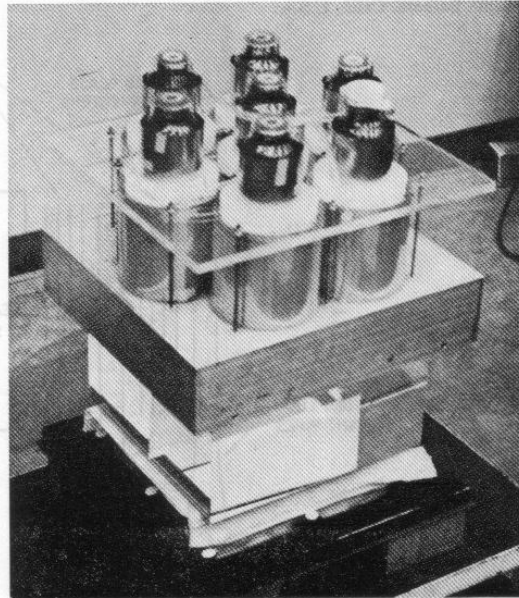
Fig. 1 shows a schematic drawing of the basic components: Since the intended use for this configuration was the detection of showers from 150 to 700 MeV, we chose a total radiator thickness of 12 radiation lengths (X^0). This is broken up into two converters/radiators ("active converters") of $2X^0$ each and a main radiator of $8X^0$ thickness, all consisting of very clear lead glass⁴). Inserted between the first and second converters, and between the second converter and the main block, there are four wire spark chamber planes each for delineation of charged particle tracks; track reconstruction in these chambers (which can be replaced by proportional wire chambers if time resolution is critical) yields the desired localization information by fixing a small fiducial volume in the converter where the photon interacted to originate the observed track(s).

To gain maximum energy information, the optical coupling of the radiators to the phototubes had to be optimized. The active converters are joined by folded light pipes to fast 5" phototubes of high quantum efficiency⁵). The main lead glass block is viewed from the back by seven 5" phototubes. For best coupling, we built a configuration of seven interlacing cones of specular aluminum, potted in casting epoxy. Fig. 2a shows this shell; it is bonded (with RTV adhesive sealant) to the lead glass block on one side and to the phototube faces on the other. The space contained inside is then filled with a clear immersion oil of an

appropriate index of refraction⁶), intermediate between that of the lead glass and that of the phototube face. Fig. 2b shows the assembly of the main block before it was encased.



(a)



(b)

Fig. 2. (a) Photographic view of interlacing aluminum cones which contain liquid light pipe; (b) main radiator block assembled with light pipe, seven 5" phototubes and bases.

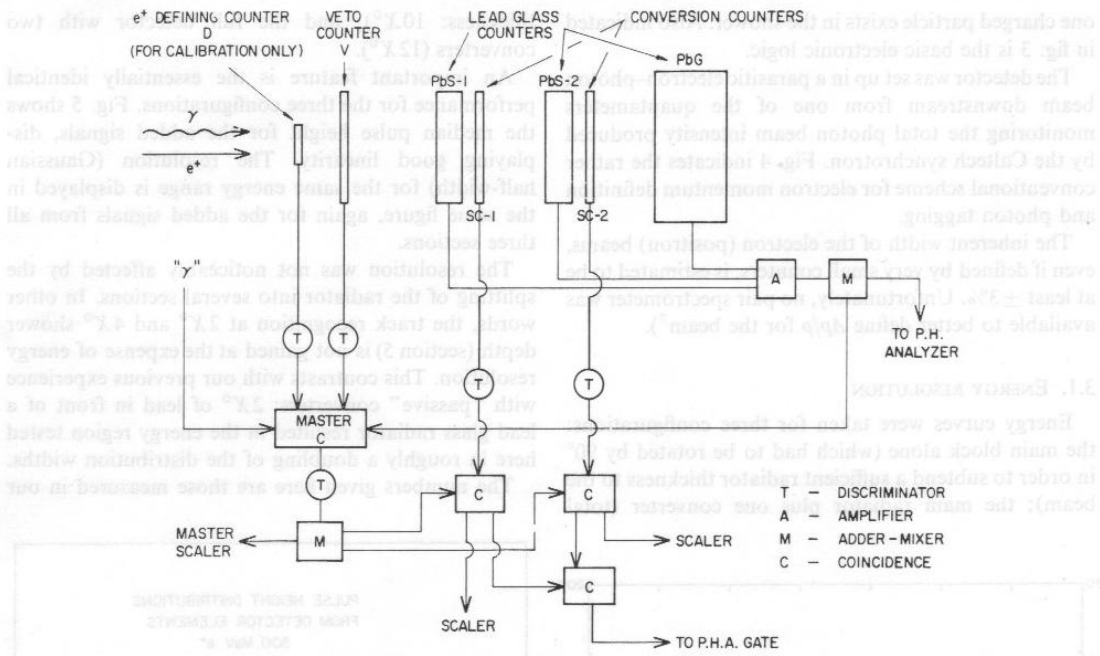


Fig. 3. Set-up of detector for tests of energy response and conversion efficiencies.

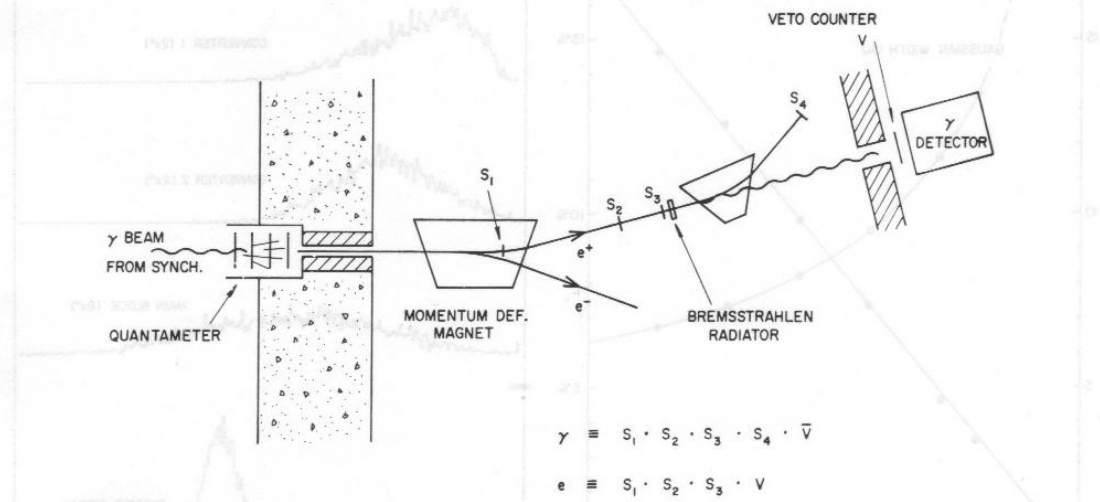


Fig. 4. Detector test set-up in parasitic electron/tagged photon beam downstream of a photon beam quantameter at the 1.5 GeV CIT electron synchrotron.

3. Counter calibrations

For calibration purposes, the detector was assembled without the spark chambers, in the configuration shown in fig. 3. A small defining counter serves for cali-

bration with incident electrons only. For photons incident, a veto counter is installed instead. The active converters are followed by scintillation counters which indicate whether, at 2X⁰ and 4X⁰, respectively, at least

one charged particle exists in the shower. Also indicated in fig. 3 is the basic electronic logic.

The detector was set up in a parasitic electron-photon beam downstream from one of the quantimeters monitoring the total photon beam intensity produced by the Caltech synchrotron. Fig. 4 indicates the rather conventional scheme for electron momentum definition and photon tagging.

The inherent width of the electron (positron) beams, even if defined by very small counters, is estimated to be at least $\pm 3\%$. Unfortunately, no pair spectrometer was available to better define $\Delta p/p$ for the beam⁷.

3.1. ENERGY RESOLUTION

Energy curves were taken for three configurations: the main block alone (which had to be rotated by 90° in order to subtend a sufficient radiator thickness to the beam); the main radiator plus one converter (total

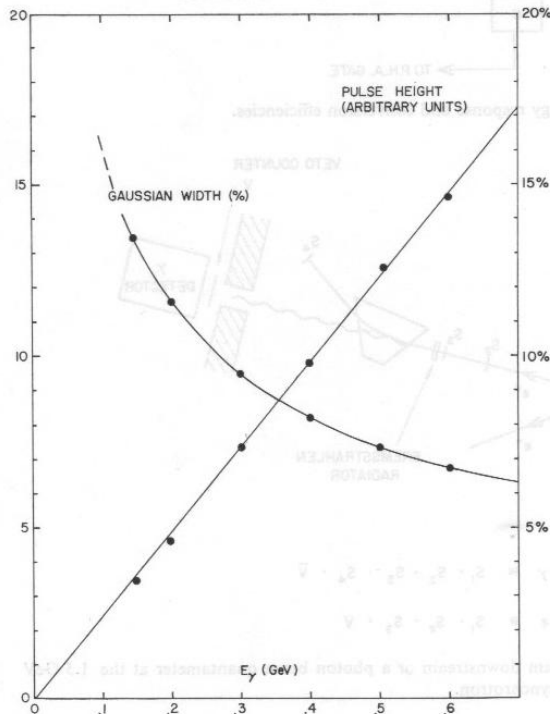


Fig. 5. Median pulse height and Gaussian width σ for pulse height distributions generated by electrons incident on detector. An estimated inherent beam width of $\approx 3\%$ has not been subtracted. Within this accuracy, the resolution was not affected by the addition of one or two converters to the main block.

thickness: $10X^0$); and the full detector with two converters ($12X^0$).

An important feature is the essentially identical performance for the three configurations. Fig. 5 shows the median pulse height for the added signals, displaying good linearity. The resolution (Gaussian half-width) for the same energy range is displayed in the same figure, again for the added signals from all three sections.

The resolution was not noticeably affected by the splitting of the radiator into several sections. In other words, the track recognition at $2X^0$ and $4X^0$ shower depth (section 5) is not gained at the expense of energy resolution. This contrasts with our previous experience with "passive" converters: $2X^0$ of lead in front of a lead glass radiator resulted in the energy region tested here in roughly a doubling of the distribution widths.

The numbers given here are those measured in our

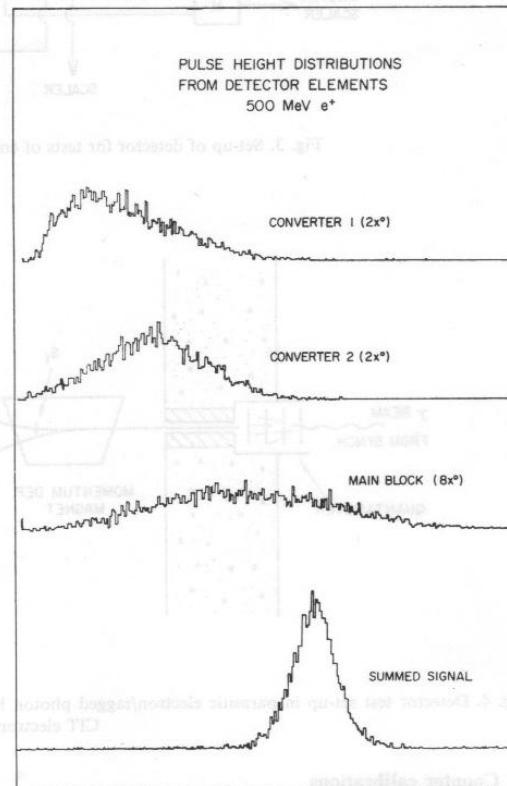


Fig. 6. Details of shower distributions: pulse heights generated in three sections of detector by 500 MeV positrons, and added signal. Note that the sum signal is on a different scale.

calibration runs, without adjustments for the inherent beam width. Within the accuracy obtainable in this way, no difference was found between the resolution due to shower absorption in one block only, and that from the added configuration.

In order to probe for inherent resolution limits, we used a light pulser to generate light flashes at the far end of the main radiator, of a median pulse height equal to that of a 500 MeV shower. In this manner, we obtained a Gaussian half-width of $\sigma(500 \text{ MeV}) \approx 4\%$, as compared with 6.7% in the actual beam. To put this number into the proper perspective, we compare it to a width of $\sigma = 10\%$ which we previously obtained in more conventional lead-glass-radiator assemblies.

3.2. DETAILED DISTRIBUTION

To study the mechanisms involved in this shower detection problem, we pulse-height-analyzed the distributions generated by individual components of the detector. It is well known that, particularly in low-energy electromagnetic cascades, the number of particles at any given depth is subject to strong statistical fluctuations⁸. This is most pronounced in the first few radiation lengths.

Fig. 6 illustrates these points for a 500 MeV shower, initiated by a positron. Distributions from the individual components of the detector clearly show the enormous fluctuation effects; the sum signal, on the other hand, is rather well defined. (Note that the sum signal is not on the same scale.) The blending of three broad and ill-defined distributions into one symmetric and narrow peak must at first glance appear remarkable.

4. Detection efficiencies

For photon track recognition, we have to make use of some portion of the tracks of charged particles close to the first vertex of the shower produced. In principle, one might sample the initial 3 or 4 radiation lengths of a shower more densely, watching out for this vertex. As a compromise between this desirable feature and the need to have converters thick enough to extract Cherenkov light generated inside, we used configurations involving $2X^0$ lead glass converters. As a function of incident photon energy, we measured the detection efficiencies of these configurations with appropriate coincidence and anticoincidence requirements.

The results are displayed in fig. 7, for energies between 0.1 and 0.6 GeV. For best track definition, it is desirable to find a charged particle track at both shower penetrations sampled ($2X^0$ and $4X^0$): curve 4 shows that the

efficiency for such full detection is exceedingly low at 100 MeV, and rises slowly to $\approx 70\%$ at 600 MeV. If we demand only one charged track in either gap, curve 3 shows a high efficiency throughout, starting at 58% for 100 MeV and rising to $\approx 96\%$ at 600 MeV. Individual detection efficiencies are also given, for $2X^0$ and $4X^0$.

5. Track delineation

The localization of the photon trajectory is effected, with an efficiency as determined in the previous section, by the wire spark chambers (or proportional chambers) inserted between the radiators. We used a set of wire chambers with 1 mm wire spacing to study the accuracy of localizing the vertices. There are two factors that influence the resolution of the detector as a track-delineating device: the inherent resolution of the track chamber ($\approx \pm 0.5 \text{ mm}$); and the angle which the charged track subtends with respect to the shower axis, together with the thickness of the converter radiator. It is important to realize that, while a spacial accuracy of order 1 mm can be achieved at the expense of either efficiency (one or a few *thin* converters) or cost (many thin converters plus track chambers), a practical compromise will have to make do with relatively thick converters, and therefore less precise localization information: while the fast component of the shower

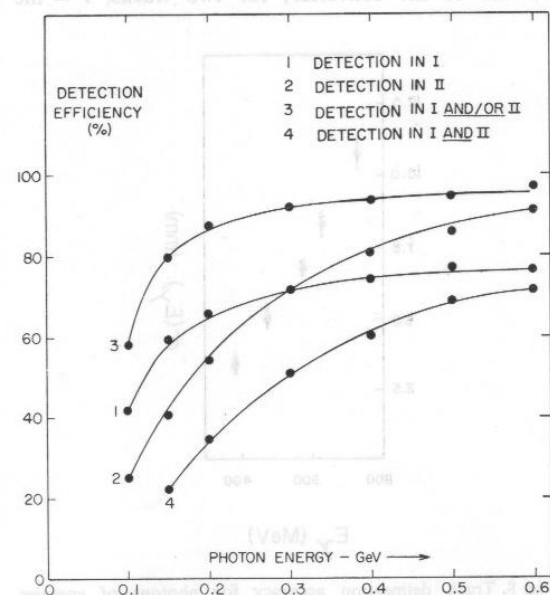


Fig. 7. Detection efficiencies as measured by insertion of scintillation counters between radiators, for various requirements.

will always be very close to the shower axis, much of the detected charged component is slow, and therefore considerably affected by multiple scattering in the "active converters".

We present a limited set of localization measurements as extracted from the data collected in an experiment⁹⁾ using these counters for final-state detection, for the critical energy range between 200 and 400 MeV (in the test beam used for the energy calibrations, no tag on photon trajectories was available). In this experiment, performed at the LBL 184" cyclotron, a small cross-section for the process $pd \rightarrow {}^3\text{He} \gamma$ had to be separated from an abundant occurrence of $pd \rightarrow {}^3\text{He} \pi^0 (\pi^0 \rightarrow 2\gamma)$. The above-described set-up was used with only one active $2X^0$ converter. We employed a set of wire chambers with 1 mm wire spacing to determine the trajectories of charged particles resulting from the photon conversion. Each track was extended to the midplane ($1X^0$ depth) of the converter, and the location of the vertex was estimated as the mean of the intersections of the tracks and the midplane. For a sample of the data with one or two tracks, we roughly estimated the uncertainty of the vertex by defining for each event the two-vector, \mathbf{r} , as follows: for one track, \mathbf{r} = the vector pointing from the estimated vertex to the point in the midplane formed by dropping a perpendicular from the point where the track intersected the surface of the converter; for two tracks, \mathbf{r} = the

vector pointing from the estimated vertex to the point where the steeper of the two tracks intersected the midplane. For a given photon energy, E , the vectors \mathbf{r} were distributed in an approximately Gaussian manner; so $r = |\mathbf{r}|$ was distributed according to:

$$\frac{d(\text{number of events})}{dr} \equiv r \exp[-r^2/2\sigma^2(E)].$$

Fig. 8 displays the observed value of $\sigma(E_\gamma)$ as function of E_γ .

It is clear that at the energies involved in this experiment, the resolution of the vertex position was limited primarily by the angle which the charged tracks subtended with respect to the shower axis, due largely to the thickness of the converter. Most charged particles are initially produced at very small angles close to the photon direction, but the visible track can be due to a large-angle Compton electron, a slow electron pair produced by a low-energy secondary photon, or an electron (positron) that has lost most of its energy from bremsstrahlung and then multiply scattered through a large angle. While the basic accuracy is of the order of 2–4 mm, it could be useful for the case of especially wide-angle tracks if a second charged track were identified at another shower depth. We have previously shown (section 3.2) that the addition of another converter can be accomplished without loss of energy resolution, and the added localization information might well be worth the price of the lower efficiency (fig. 7).

We stress again that with increasing energy, and particularly in the multi-GeV region, these problems diminish rapidly.

6. Conclusion

We conclude that the detector described here represents a reasonable compromise towards fulfilling most of the requirements expected from a hodoscope/spectrometer for intermediate energy photons, and may be close to optimal when used at high energies.

Essential features are

- the combined-function converters/radiators ("active" converters), allowing for efficient photon conversion for track delineation, while maintaining the basic energy resolution of the device;
- track delineation close to the initial shower vertex, with accuracies only fair in the 150–400 MeV range, but improving with energy and limited ultimately only by the inherent resolution of the track recognition in the spark chambers;
- track delineation efficiencies depending on the

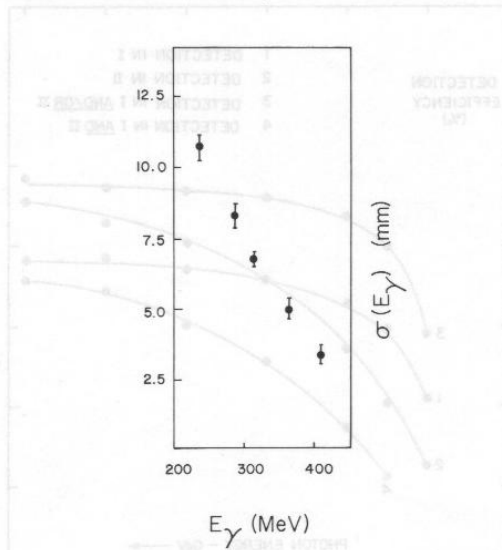


Fig. 8. Track delineation accuracy for photons of energies $150 \leq E_\gamma \leq 350$ MeV, as extracted from a completed experiment. Uncertainties are almost entirely due to multiple scatters and slow secondaries; improves rapidly with energy.

photon energies, but rapidly increasing up to $\lesssim 1$ GeV, and essentially constant above this energy;

- d) full photon detection and energy absorption irrespective of track delineation efficiency;
- e) easy adaptability of geometries and radiator and detector materials to requirements dictated by experiment needs; easy scaling with energy, up to very high energies.

It is a pleasure to thank W. Nilsson and W. Friedler for their inventiveness and excellent workmanship, which helped to overcome all technological problems. We also thank A. Neubieser and the Cal Tech synchrotron operators and crew as well as J. Vale and the LBL 184" cyclotron operators; without their unfailing help this detector could not have been tested in the last days of the Cal Tech synchrotron operation, or used in the LBL experiment. We also thank C. Prescott for his help on the initial stages of this work.

References

- 1) This energy range was dictated by the requirements of a particular experiment, where the final states ${}^3\text{He } \gamma$ and ${}^3\text{He } \pi^0$ had to be separated in a time reversal invariance test using the reactions $p d \leftrightarrow {}^3\text{He } \gamma$.
- 2) At very high energies ($\gtrsim 100$ GeV), it may be perfectly satisfactory to form the main body of the detector out of less costly materials than the lead glass used here. Cf. C. A. Heusch, NAL Summer Study Report (1969) vol. 3, p. 51.
- 3) A design report was presented to the Intern. Conf. on *Instrumentation in high energy physics* (Dubna, USSR, 1970) (C. A. Heusch, R. V. Kline, C. Y. Prescott and S. J. Yellin, Caltech Report CALT-68-255).
- 4) Schott Optical Company, lead glass SF-5. Technical data: $\rho = 4.08$ g/cm³, $lX^0 = 2.36$ cm, index of refraction: $n = 1.6727$. Sizes of the converter blocks: $25.4 \times 26.3 \times 4.83$ cm³; of the main block: $33.3 \times 34.5 \times 19.0$ cm³.
- 5) For the converters/radiators we used experimental multi-alkalide photocathode tubes, RCA C70133A; for the main radiator, bi-alkali tubes, RCA 4522.
- 6) Index of Refraction Liquids, R. P. Curgille Laboratories, Inc., Cedar Grove, New Jersey. Available from $n_D = (1.300-1.395) \pm 0.0005$, $n_D = (1.400-1.700) \pm 0.0002$.
- 7) Also, the device was tested in the last days before the Caltech synchrotron was definitively shut down, thus limiting the time available for beam-improvement work.
- 8) J. Butcher and H. Messel, Nucl. Phys. **38** (1962) 1; for an experimental investigation of these features, see, e.g., C. A. Heusch and C. Y. Prescott, Phys. Rev. **135** (1964) B772.
- 9) C. A. Heusch, R. V. Kline, K. T. McDonald, J. Carroll, D. H. Fredrickson, M. B. Goitein, B. MacDonald, V. Perez-Mendez and A. W. Stetz (UCSC # 73-005 and # 73-008, 1973, to be published).